

Observation of swell dissipation across oceans

Fabrice Ardhuin,¹ Bertrand Chapron,² and Fabrice Collard³

Received 31 December 2008; revised 14 February 2009; accepted 23 February 2009; published 27 March 2009.

[1] Global observations of ocean swell, from satellite Synthetic Aperture Radar data, are used to estimate the dissipation of swell energy for a number of storms. Swells can be very persistent with energy e-folding scales exceeding 20,000 km. For increasing swell steepness this scale shrinks systematically, down to 2800 km for the steepest observed swells, revealing a significant loss of swell energy. This value corresponds to a normalized energy decay in time $\beta = 4.2 \times 10^{-6} \text{ s}^{-1}$. Many processes may be responsible for this dissipation. The increase of dissipation rate in dissipation with swell steepness is interpreted as a laminar to turbulent transition of the boundary layer, with a threshold Reynolds number of the order of 100,000. These observations of swell evolution open the way for more accurate wave forecasting models, and provide a constraint on swell-induced air-sea fluxes of momentum and energy.

Citation: Ardhuin, F., B. Chapron, and F. Collard (2009), Observation of swell dissipation across oceans, *Geophys. Res. Lett.*, 36, L06607, doi:10.1029/2008GL037030.

1. Introduction

[2] Swells are surface waves that outrun their generating wind, and radiate across ocean basins. At distances of 2000 km and more from their source, these waves closely follow principles of geometrical optics, with a constant wave period along geodesics, when following a wave packet at the group speed [e.g., *Snodgrass et al.*, 1966; F. Collard et al., Persistence of ocean swell fields observed from space, submitted to *Journal of Geophysical Research*, 2008]. These geodesics are great circles along the Earth surface, with minor deviations due to ocean currents.

[3] Because swells are observed to propagate over long distances, their energy should be conserved or weakly dissipated [*Snodgrass et al.*, 1966], but little quantitative information is available on this topic. As a result, swell heights are relatively poorly predicted [e.g., *Rogers*, 2002; *Rascle et al.*, 2008]. Numerical wave models that neither account specifically for swell dissipation, nor assimilate wave measurements, invariably overestimate significant wave heights (H_s) in the tropics. Typical biases in such models reach 45 cm or 25% of the mean observed wave height in the East Pacific [*Rascle et al.*, 2008]. Further, modelled peak periods along the North American west coast exceed those measured by open ocean buoys, on average by 0.8 s [*Rascle et al.*, 2008], indicating an excess of long

period swell energy. Theories proposed so far for nonlinear wave evolution or air-sea interactions [e.g., *Watson*, 1986; *Tolman and Chalikov*, 1996], require order-of-magnitude empirical corrections in order to produce realistic wave heights [e.g., *Tolman*, 2002]. Swell evolution over large scales is thus not understood.

[4] Swells are also observed to modify air-sea interactions [*Grachev and Fairall*, 2001], and swell energy has been suggested as a possible source of ocean mixing [*Babanin*, 2006]. A quantitative knowledge of the swell energy budget is thus needed both for marine weather forecasting and Earth system modelling.

[5] The only experiment that followed swell evolution at oceanic scales was carried out in 1963. Using in situ measurements, a very uncertain but moderate dissipation of wave energy was found [*Snodgrass et al.*, 1966]. The difficulties of this type of analysis are twofold. First, very few storms produce swells that line up with any measurement array, and second, large errors are introduced by having to account for island sheltering. Qualitative investigations by *Holt et al.* [1998] and *Heimbach and Hasselmann* [2000] demonstrated that a space-borne synthetic aperture radar (SAR) could be used to track swells across the ocean, using the coherent persistence of swells along their propagation tracks. Building on these early studies, Collard et al. (submitted manuscript, 2008) demonstrated that SAR-derived swell heights can provide estimates of the dissipation rate. Here we make a systematic and quantitative analysis of four years of global SAR measurements, using level 2 wave spectra [*Chapron et al.*, 2001] from the European Space Agency's (ESA) ENVISAT satellite. The swell analysis method is briefly reviewed in section 2. The resulting estimates of swell dissipation rates are interpreted in section 3, and conclusions follow in section 4.

2. Swell Tracking and Dissipation Estimates

[6] Our analysis uses a two step method. Firstly, using SAR-measured wave periods and directions at different times and locations, we follow great circle trajectories backwards at the theoretical group velocity. The location and date of a swell source is defined as the spatial and temporal center of the convergence area and time of the trajectories. We define the spherical distance α from this storm center ($\alpha = X/R$ where X is the distance along the surface on a great circle, and R is the Earth radius).

[7] Secondly, we chose a wave period T and, starting from the source at time $t = 0$ and an angle θ_0 , we follow imaginary wave packets along the great circle at the group speed $C_g = gT/(4\pi)$. SAR data are retained if they are acquired within 3 hours and 100 km from the theoretical position of our imaginary wave packet, and if a swell partition is found with peak wavelength and direction within

¹Service Hydrographique et Océanographique de la Marine, Brest, France.

²Ifremer, Laboratoire d'Océanographie Spatiale, Centre de Brest, Plouzané, France.

³Collecte Localisation Satellites, Division Radar, Plouzané, France.

50 m and 20° of their expected values. This set of SAR observations constitutes one swell track. We repeat this procedure by first varying θ_0 . Tracks with neighboring values of θ_0 are merged in relatively narrow direction bands (5 to 10° wide) in order to increase the number of observations along a track. This ensemble of tracks is the basic data set used in our analysis. Such track ensembles are produced for different storms and different wave periods. Because the SAR sampling must match the natural swell propagation, ten storms only produced 22 track ensembles with enough SAR data that satisfies our selection criteria in the period 2003 to 2007 (see auxiliary material).¹ These criteria are wind speeds less than 9 m s^{-1} , swell heights larger than 0.5 m , and the observations should span more than 3000 km along the great circle, in order to produce a stable estimate of the swell spatial decay rate μ .

[8] In the absence of dissipation (i.e., $\mu = 0$), Collard et al. (submitted manuscript, 2008) demonstrated that, in any chosen direction θ_0 and at the spherical distance α and time t corresponding to a propagation at a chosen group speed C_g , the swell energy E_s decreases asymptotically as $1/[\alpha \sin(\alpha)]$. The $\sin(\alpha)$ factor arises from the initial spatial expansion of the energy front, with a narrowing of the directional spectrum. The α factor is due to the dispersive spreading of the energy packet, because C_g is proportional to T , associated to a narrowing of the frequency spectrum. Collard et al. (submitted manuscript, 2008) also showed that for realistic wave conditions E_s should be within 20% of the asymptotic values for distances αR larger than 4000 km from the storm center, where R is the Earth radius. In our estimation of μ , data within 4000 km of the originating storm are ignored to make sure that the remaining data are in the far field of the storm.

[9] This 4000 km value was estimated for a storm of radius $r = 1000 \text{ km}$. This applies to any storm provided that all the energy for the wave period T is confined within this radius at $t = 0$, with no generation of such long swells for $t > 0$. Fast moving and long-lived storms may lead to larger values of r and, following Collard et al. (submitted manuscript, 2008), deviations from the asymptote larger than 20%. An extreme situation would be a steady storm moving along the great circle at the speed C_g , that would generate a constant swell energy E_s as a function of α . No such situation was found in the storms analyzed below.

[10] In each track ensemble, all swells have close initial directions θ_0 , and the wave field is only a function of α . We define the spatial evolution rate

$$\mu = -\frac{d(\alpha \sin \alpha E_s)/d\alpha}{R(\alpha \sin \alpha E_s)}. \quad (1)$$

Positive values of μ correspond to losses of wave energy (Figure 1a). Negative, but not significant, values are occasionally found (Figure 1b).

[11] For each track ensemble we take a reference distance $\alpha_0 = \pi/5$ which corresponds to 4000 km . μ is estimated by finding the pair $(\hat{E}_s(\alpha_0), \mu)$, that minimizes the mean square difference between observed swell energies $E_s(\alpha_i)$ with i

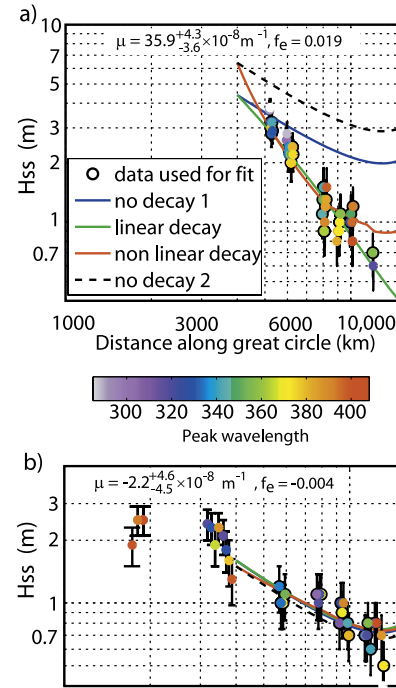


Figure 1. Observed swell wave height as a function of distance, and theoretical decays with fitted constant coefficients using no dissipation, linear (μ constant) or non-linear (f_e constant) dissipation for the 15 s waves generated by (a) a very strong North Pacific storm on 12 February 2007 (Table S1: swell number 18) and (b) a weaker southern ocean storm on 12 August 2007 (Table S1: swell number 19). Circled dots are the observations used in the fitting procedure. Error bars show one standard deviation of the expected error on each SAR measurement (Collard et al., submitted manuscript, 2008).

ranging from 1 to N , and the theoretical constant linear decay,

$$\hat{E}_s(\alpha_i) \alpha_i \sin \alpha_i = \hat{E}_s(\alpha_0) \alpha_0 \sin \alpha_0 e^{-R\mu(\alpha_i - \alpha_0)}. \quad (2)$$

Because we only have two parameters μ and $\hat{E}_s(\alpha_0)$ to adjust, the minimization is performed by a complete search of the parameter space.

[12] Collard et al. (submitted manuscript, 2008) estimated that the SAR-derived swell heights $H_{ss} = 4\sqrt{E_s}$ are gamma-distributed about a true value $H_{ss} - b_H$. The bias is well approximated by

$$b_H = 0.11 + 0.1H_{ss} - 0.1 \max\{0, U_{10SAR} - 7\} \quad (3)$$

with H_{ss} in meters and the wind speed U_{10} in m s^{-1} . A realistic model of the standard deviation of the measurement error is

$$\sigma_H = 0.10 \text{ m} + \min\{0.25H_{ss}, 0.8 \text{ m}\}. \quad (4)$$

[13] Using this error model, we generated 400 synthetic data sets by perturbing independently each measured swell wave height, in order to obtain a confidence interval for μ .

¹Auxiliary materials are available in the HTML. doi:10.1029/2008GL037030.

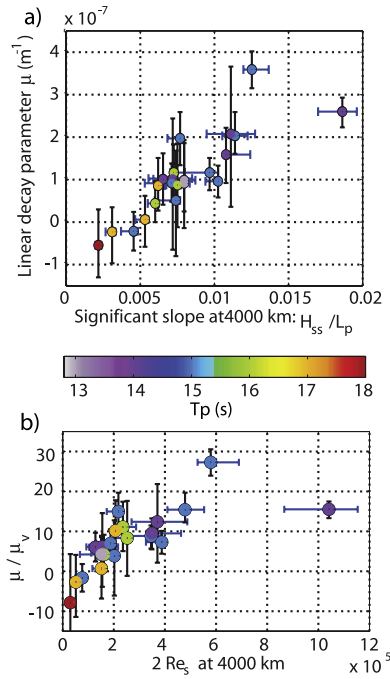


Figure 2. Swell dissipation for 22 events (see auxiliary material for details). (a) Estimated linear attenuation coefficient as a function of the initial significant slope, ratio of the swell significant wave height and peak wavelength, $s = 4 H_s/L$, taken 4000 km from the storm centre, for a variety of peak swell periods (colors). (b) Attenuation coefficient normalized by the viscous attenuation μ_v (equation (5)) as a function of the significant swell Reynolds number Re_s , determined from significant velocity and displacement amplitudes at 4000 km from the storm.

For each swell case, the values of μ and $H_{ss}(\alpha_0)$ reported below are the medians of the 400 calculated values.

[14] For all our swell data, μ ranges from -0.6 to $3.7 \times 10^{-7} \text{ m}^{-1}$ (Figure 2a), comparable to $2.0 \times 10^{-7} \text{ m}^{-1}$ previously reported for large amplitude swells with a 13 s period [Snodgrass *et al.*, 1966]. Clarifying earlier observations by Darbyshire [1958] and Snodgrass *et al.* [1966], our analysis unambiguously proves that swell dissipation increases with the wave steepness. We recall that, in the absence of dissipation, a maximum 20% deviation of E_s relative to the asymptote is expected due to the storm shape. This deviation is equal to the one produced by a real $5.0 \times 10^{-8} \text{ m}^{-1}$ dissipation over 4000 km. Thus a comparable error on the estimation of μ is expected when, as we do here, the storm shape is not taken into account (Collard *et al.*, submitted manuscript, 2008).

3. Interpretation of Swell Dissipation

[15] At present there is no consensus on the plausible causes of the loss of swell energy [WISE Group, 2007]. Interaction with oceanic turbulence is expected to be relatively small [Ardhuin and Jenkins, 2006]. Observed modifications and reversals of the wind stress over swells [Grachev and Fairall, 2001] suggest that some swell momentum is lost to the atmosphere. The wave-induced modulations of air-sea stresses yield a flux of energy from

the waves to the wind, due to the correlations of pressure and velocity normal to the sea surface, and the correlations of shear stress and tangential velocity. An upward flux of momentum, readily observed over steep laboratory waves, can thus result in a wave-driven wind [Harris, 1966]. If these modulations are linearized [e.g., Kudryavtsev and Makin, 2004], the swell dissipation rate becomes linear in terms of the wave energy, with a proportionality constant that typically depends on the wind, but which does increase with the swell steepness, as we observe here.

[16] Our observations show no clear trend with wind magnitude U_{10} and wind-wave angle θ_w : the swell age C/U_{10} or $C/(U_{10} \cos \theta_w)$ averaged over the swell track gives little correlation with μ , even when weighted with the swell energy. We thus take a novel approach, and interpret our data by neglecting the effect of the wind, considering only the shear stress modulations induced by swell orbital velocities. Little data are available for air flows over swells, but boundary layers over fixed surfaces are well known, and should have similar properties if their significant orbital amplitudes of velocity and displacement are doubled (Collard *et al.*, submitted manuscript, 2008). The dissipation then depends on the surface roughness and a significant Reynolds number, $Re(\phi) = 4u_{orb}(\phi)a_{orb}(\phi)/\nu$, where u_{orb} and a_{orb} are the significant amplitudes of the surface orbital velocities and displacements.

[17] For $Re < 10^5$, the flow should be laminar [Jensen *et al.*, 1989]. The strong shear above the surface makes the air viscosity important, with a dissipation coefficient given by [Dore, 1978; Collard *et al.*, submitted manuscript, 2008]

$$\mu_v = 2 \frac{\rho_a}{\rho_w g C_g} \left(\frac{2\pi}{T} \right)^{5/2} \sqrt{2\nu}, \quad (5)$$

where L is the swell wavelength, $L = gT^2/(2\pi)$ in deep water with g the acceleration of gravity. At ambient temperature and pressure, the air viscosity is $\nu = 1.4 \times 10^{-5} \text{ m}^2 \text{ s}^{-1}$, and μ_v is only a function of T . As T increases from 13 to 19 s, μ_v decreases from 2.2×10^{-8} to $5.8 \times 10^{-9} \text{ m}^{-1}$.

[18] For larger Reynolds numbers the flow becomes turbulent. The energy rate of decay in time can be written as

$$\beta = -\frac{dE_s/dt}{E_s} = C_g \mu = \frac{\rho_a 4\pi^2}{\rho_w g T^2} f_e u_{orb} \quad (6)$$

where f_e is a swell dissipation factor. For a smooth surface, f_e is of the order of 0.002 to 0.008 [Jensen *et al.*, 1989], when assumed equal to the friction factor f_w .

[19] Re is difficult to estimate from the SAR data only, because ENVISAT's ASAR does not resolve the short wind-sea waves. However, in deep water we can define the smaller 'swell Reynolds number' Re_s from $u_{orb,s} = 2\sqrt{E_s}2\pi/T$ and $a_{orb,s} = 2\sqrt{E_s}$.

[20] Our estimates of μ exceed μ_v by a factor that ranges from $O(1)$ to 28 (Figure 2b), quantitatively similar to oscillatory boundary layer over fixed surfaces with no or little roughness. Namely, dissipation rates μ of the order of the viscous value μ_v are found for $Re_s < 5 \times 10^4$ when the flow may be laminar, and we only find large values of μ/μ_v when $Re_s > 5 \times 10^4$ over a significant portion of the swell track. For reference, a 6.3 m s^{-1} wind can generate

a fully-developed wind-sea with $Re = 2 \times 10^5$, making the boundary layer turbulent for any swell amplitude. Using the numerical wave model described by F. Ardhuin et al. (Observation and estimation of Lagrangian, Stokes and Eulerian currents induced by wind and waves at the sea surface, submitted to *Journal of Physical Oceanography*, 2009), one finds that this value of Re_s translates to $Re \simeq 10^5$. That same model also gives values of u_{orb} . Fitting a constant f_e for each track ensemble yields $-0.001 \leq f_e \leq 0.019$, with a median of 0.007, close to what is expected over a smooth surface. This suggests that the roughness of the waves for this oscillatory motion is very small compared to the orbital amplitude.

[21] A parameterization of swell dissipation, taking f_e constant in the range 0.0035 to 0.007, generally yields accurate wave heights (not shown). The quality of the end result also depends on the other parameterizations for wind input, whitecapping and wave-wave interactions, and requires a rather lengthy discussion [e.g., Ardhuin et al., 2008, also submitted manuscript, 2009].

[22] Beyond this simple model, we expect that winds should modify the boundary layer over swell, with a significant effect for winds larger than 7 m s^{-1} (Collard et al., submitted manuscript, 2008). Kudryavtsev and Makin [2002] considered the wind stress modulations due to short wave roughness modulated by swells, and found that the preferential breaking of short waves near long wave crests could double the wind-wave coupling coefficient μ for the long waves. Yet, their linear model cannot explain the nonlinear dissipation observed here, because they only considered lowest order effects. Further investigations should probably consider both wind and finite amplitude swell effects to explain the observed variability of μ .

[23] If this dissipation is due to the proposed air-sea friction mechanism, the associated momentum flux $\rho_w g E_s / 2$ goes to the atmosphere. If, on the contrary, underwater processes dominate, an energy flux $\rho_w g C_g E_s$ may go into ocean turbulence. Accordingly, these fluxes are small. For 3 m high swells, the momentum flux is 8% of the wind stress produced by a 3 m s^{-1} wind. This momentum flux thus plays a minor role in observed O(50%) modifications of the wind stress at low wind [Drennan et al., 1999; Grachev and Fairall, 2001]. Wind stress modifications are more likely associated with a nonlinear influence of swell on turbulence in the atmospheric boundary layer [Sullivan et al., 2008]. This effect may arise as a result of the low-level wave-driven wind jet [Harris, 1966] and its effects on the wind profile around the critical level for the short wave generation [Hristov et al., 2003]. Whatever the actual process, the dissipation coefficient μ is a key parameter for validating theoretical and numerical models [Kudryavtsev and Makin, 2004; Hanley and Belcher, 2008].

4. Conclusions

[24] Using high quality data from a space-borne synthetic aperture radar, ocean swells were systematically tracked across ocean basins over the years 2003 to 2007. Ten storms provided enough data to allow a total of 22 estimations of the swell energy budget for peak periods of 13 to 18 s. The dissipation of small-amplitude swells is not distinguishable from viscous dissipation, with decay scales larger than

20000 km. On the contrary, steep swells lose a significant fraction of their energy, up to 65% over a distance as short as 2800 km. This non-linear behavior is consistent with a transition from a laminar to a turbulent air-side boundary layer. Many other processes may contribute to the observed dissipation, and a full model of the air-sea interface will be needed for further progress. The present observations and analysis opens the way for a better understanding of air-sea fluxes in low wind conditions, and more accurate hindcasts and forecasts of sea states [see Ardhuin et al., 2008, also submitted manuscript, 2009] (and, e.g., the SHOM results by Bidlot [2008]).

[25] Further investigations are necessary to understand the wind stress modulations and their variations with wind speed, direction, and swell amplitude. Such an effort is essential for the improvement of numerical wave models and their application to remote sensing and the estimation of air-sea fluxes.

[26] **Acknowledgments.** SAR data were provided by the European Space Agency (ESA). The swell decay analysis was funded by the French Navy as part of the EPEL program. This work is a contribution to the ANR-funded project HEXECO and DGA-funded project ECORS.

References

- Ardhuin, F., and A. D. Jenkins (2006), On the interaction of surface waves and upper ocean turbulence, *J. Phys. Oceanogr.*, **36**, 551–557.
- Ardhuin, F., F. Collard, B. Chapron, P. Queffelecoulou, J.-F. Filipot, and M. Hamon (2008), Spectral wave dissipation based on observations: A global validation, in *Proceedings of Chinese-German Joint Symposium on Hydraulics and Ocean Engineering*, edited by U. Zanke, pp. 391–400, Tech. Univ. Darmstadt, Darmstadt, Germany.
- Babanin, A. V. (2006), On a wave-induced turbulence and a wave-mixed upper ocean layer, *Geophys. Res. Lett.*, **33**, L20605, doi:10.1029/2006GL027308.
- Bidlot, J.-R. (2008), Intercomparison of operational wave forecasting systems against buoys: data from ECMWF, MetOffice, FNMOC, NCEP, DWD, BoM, SHOM and JMA, September 2008 to November 2008, technical report, Joint WMO-IJC Tech. Comm. for Oceanogr. and Mar. Meteorol., Paris. (Available at <http://preview.tinyurl.com/7b26jj>)
- Chapron, B., H. Johnsen, and R. Garelo (2001), Wave and wind retrieval from SAR images of the ocean, *Ann. Telecommun.*, **56**, 682–699.
- Darbyshire, J. (1958), The generation of waves by wind, *Philos. Trans. R. Soc. London, Ser. A*, **215**, 299–428.
- Dore, B. D. (1978), Some effects of the air-water interface on gravity waves, *Geophys. Astrophys. Fluid. Dyn.*, **10**, 215–230.
- Drennan, W. M., H. C. Graber, and M. A. Donelan (1999), Evidence for the effects of swell and unsteady winds on marine wind stress, *J. Phys. Oceanogr.*, **29**, 1853–1864.
- Grachev, A. A., and C. W. Fairall (2001), Upward momentum transfer in the marine boundary layer, *J. Phys. Oceanogr.*, **31**, 1698–1711.
- Hanley, K. E., and S. E. Belcher (2008), Wave-driven wind jets in the marine atmospheric boundary layer, *J. Atmos. Sci.*, **65**, 2646–2660.
- Harris, D. L. (1966), The wave-driven wind, *J. Atmos. Sci.*, **23**, 688–693.
- Heimbach, P., and K. Hasselmann (2000), Development and application of satellite retrievals of ocean wave spectra, in *Satellites, Oceanography and Society*, edited by D. Halpern, pp. 5–33, Elsevier, Amsterdam.
- Holt, B., A. K. Liu, D. W. Wang, A. Gnanadesikan, and H. S. Chen (1998), Tracking storm-generated waves in the northeast Pacific Ocean with ERS-1 synthetic aperture radar imagery and buoys, *J. Geophys. Res.*, **103**, 7917–7929.
- Hristov, T. S., S. D. Miller, and C. A. Friehe (2003), Dynamical coupling of wind and ocean waves through wave-induced air flow, *Nature*, **422**, 55–58.
- Jensen, B. L., B. M. Sumer, and J. Fredsøe (1989), Turbulent oscillatory boundary layers at high Reynolds numbers, *J. Fluid Mech.*, **206**, 265–297.
- Kudryavtsev, V. N., and V. K. Makin (2002), Coupled dynamics of short waves and the airflow over long surface waves, *J. Geophys. Res.*, **107**(C12), 3209, doi:10.1029/2001JC001251.
- Kudryavtsev, V. N., and V. K. Makin (2004), Impact of swell on the marine atmospheric boundary layer, *J. Phys. Oceanogr.*, **34**, 934–949.
- Rascle, N., F. Ardhuin, P. Queffelecoulou, and D. Croizé-Fillon (2008), A global wave parameter database for geophysical applications. Part 1:

- Wave-current-turbulence interaction parameters for the open ocean based on traditional parameterizations, *Ocean Modell.*, **25**, 154–171, doi:10.1016/j.ocemod.2008.07.006.
- Rogers, W. E. (2002), An investigation into sources of error in low frequency energy predictions, *Tech. Rep. Formal Rep. 7320-02-10035*, Oceanogr. Div. Nav. Res. Lab., Stennis Space Center, Miss.
- Snodgrass, F. E., G. W. Groves, K. Hasselmann, G. R. Miller, W. H. Munk, and W. H. Powers (1966), Propagation of ocean swell across the Pacific, *Philos. Trans. R. Soc. London, Ser. A*, **249**, 431–497.
- Sullivan, P. P., J. B. Edson, T. Hristov, and J. C. McWilliams (2008), Large-eddy simulations and observations of atmospheric marine boundary layers above nonequilibrium surface waves, *J. Atmos. Sci.*, **65**, 1225–1244.
- Tolman, H. L. (2002), Validation of WAVEWATCH-III version 1.15, *Tech. Note 213*, 33 pp., U.S. Dep. of Comm., Washington, D. C.
- Tolman, H. L., and D. Chalikov (1996), Source terms in a third-generation wind wave model, *J. Phys. Oceanogr.*, **26**, 2497–2518.
- Watson, K. M. (1986), Persistence of a pattern of surface gravity waves, *J. Geophys. Res.*, **91**, 2607–2615.
- WISE Group (2007), Wave modelling the state of the art, *Prog. Oceanogr.*, **75**, 603–674, doi:10.1016/j.pocean.2007.05.005.
-
- F. Ardhuin, Service Hydrographique et Océanographique de la Marine, F-29609 Brest, France. (ardhuin@shom.fr)
- B. Chapron, Laboratoire d’Océanographie Spatiale, Ifremer, Centre de Brest, F-29280 Plouzané, France. (bertrand.chapron@ifremer.fr)
- F. Collard, Collecte Localisation Satellites, Division Radar, F-29280 Plouzané, France. (dr.fab@cls.fr)